

Improved Integrated Launch Package Ballistic Performance

Alexander E. Zielinski and Paul Weinacht

U.S. Army Research Laboratory, Aberdeen Proving Ground, Maryland 21005-5066

Abstract— A detailed experimental investigation of the launch and flight performance of a kinetic energy fin-stabilized penetrator has been performed. The Integrated Launch Package (ILP) consists of the subprojectile and mid-riding armature. The armature front contact is electrically insulated from the rails. This configuration has shown potential for effectively managing the launch disturbances. To evaluate the transitional ballistics, aeroballistics, and jump characteristics, single-shot firings with an exit velocity of 1,350 m/s were conducted at the ARL Transonic Experimental Facility, APG, MD. The impact data show larger variability in the vertical direction than in the horizontal direction. Results from the jump survey indicate that effects of the deviation from the launcher centerline (i.e., straightness) contribute significantly to the target impact dispersion. Substantial contributions from the linear and angular rates at the muzzle are evident in the vertical direction. The contribution attributable to sabot discard in either plane is minimal. When possible, comparisons are made to our earlier investigation which examined the ballistic behavior of a similar ILP with a conducting front contact.

Index Terms— Accuracy, Dispersion, Jump Test, Launch Dynamics

I. INTRODUCTION

In the projected battlefield environment, weapon systems that can function at velocities above conventional ordnance velocity offer many benefits to the combat system.[1] However, for all but the simplest targets, the level of incapacitation is related to the subprojectile accuracy. Thus, using electromagnetics to increase the launch velocity without regard to the propulsion environment can result in a deficient system. The primary objective of this work was to suggest improvements to enhance the integrated launch package (ILP) accuracy and then verify the design modifications through experiments. In a related study, experimental conditions were identified that led to the improvement in accuracy for a similar caliber subprojectile.[2] The mechanisms for improvement include the armature current profile and the armature front contact stiffness. In this paper, these results were implemented us-

ing the Cannon-Caliber Electromagnetic Gun (CEMG) launcher[3] and ILP.[4] This hardware has been extensively tested in prior work and was found to be robust and reliable for such an experimental investigation. The launcher is a series-augmented launcher 2.25 m long with a rectangular bore cross-section (17 mm \times 39 mm) and is identical in construction to that used in previous work.[4] However, as with conventional launch tubes, significant differences in the deviation from the bore centerline (i.e., straightness) were present. The ILP weighs 180 g (90-g armature, 90-g subprojectile) and is launched at 1,350 m/s. The armature is a two-piece design with the separation plane in the vertical direction. The armature makes contact with the rail surface in two distinct locations. In previous work, the front contact was integral with the aluminum mid-section. In this effort, the ILP's front contact was machined smaller than the rail-to-rail dimension and fitted with a polyethylene insert (i.e., insulating) to make contact with the rail surface. The insulated front contact (IFC) provides for a less stiff front bore riding surface in the vertical direction. The subprojectile length is nominally 175 mm with the center of gravity (cg) 85 mm behind the nose. A photograph of a similar style IFC ILP is shown in Fig. 1.

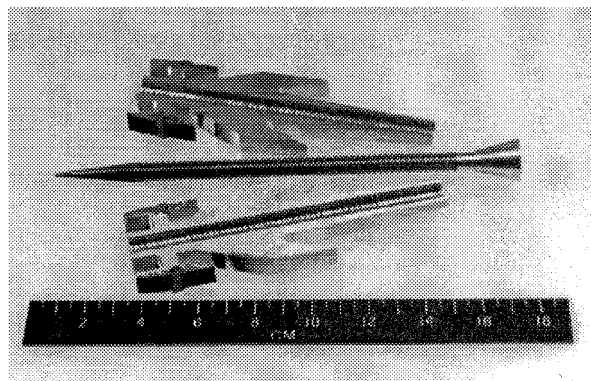


Fig. 1. Example of an IFC ILP from Reference 2

The flight path of the subprojectile, and hence the accuracy and dispersion, is influenced by the series of launch disturbances leading to free flight. A jump test is used to quantify the effects of the various disturbances imparted to the subprojectile. The contribution from each disturbance toward the subprojectile dispersion is then deter-

Manuscript received May 1, 1998.

A. Zielinski, E-mail: zielinsk@arl.mil, Fax: 410-278-2460; P. Weinacht, E-mail: weinacht@arl.mil.

mined.

The organization of this paper is as follows: In Sec. II, the experimental conditions are described. In Sec. III, the acquisition of the aerodynamic data and their use in evaluating the models are described. In Sec. IV, the jump survey is described and its components evaluated. Finally, Sec. V contains our summary and conclusions.

II. EXPERIMENT

A capacitor bank was used to provide energy to the launcher. Results from a prior study indicated that a conducting front contact armature configuration had slightly better ballistic performance when the armature current was reduced just before exit.[2] Also, large currents at ILP exit were found to have deleterious effects on the muzzle.[3] To satisfy both requirements, an explosively activated closing switch was connected across the launcher rails at the muzzle. The switch was closed just before exit. Representative current traces for the launcher (solid line) and muzzle switch (dashed line) are shown in Fig. 2.

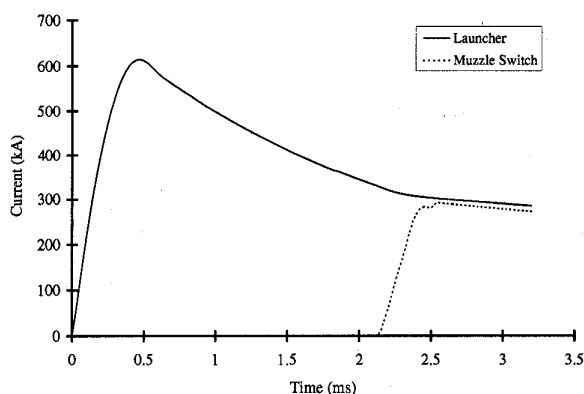


Fig. 2. Currents for shot 12.

For this shot, the initial charge voltage is 7.2 kV and the muzzle switch was closed at 2.14 ms. A peak current of 615 kA is reached at 0.46 ms. The ILP exits the launcher at 2.44 ms with a muzzle velocity of 1,350 m/s. At this time, the armature current is commutated to 14 kA while the launcher is carrying 302 kA. The efficiency of the launcher is 30% and the overall system efficiency is 20.5%. Unlike previous work, the initial test conditions for this survey remained fixed. The average peak current for the jump test was 615 kA, ± 2 kA. The average launch velocity determined from the multistation flash x-ray images was 1,351 m/s, ± 10 m/s. Other electrical data acquired during the shot include the breech, launcher, and muzzle voltages. The voltage data and previous analysis indicate that the rear armature contact transitioned.[5] While this certainly plays an important role in ILP performance, the entire jump test was conducted with a transitioned rear contact.

The launcher was firmly bolted to a steel frame at the breech end and supported 0.6 m from the muzzle end. The

steel support frame was bolted to a steel channel embedded in the concrete floor. Prior to ILP testing, the muzzle was monitored for movement with an electro-optical device (Optron) and a high speed camera (Hycam). While the Optron did not function in the EM environment, deflection measurements made by striking the muzzle with a hammer showed peak deflections less than 25 μm . The high speed camera was focused on the edge of a plate, firmly attached to the muzzle, and a stationary reference bar. Several tens of μm of displacement are discernible in the field of view. Before the jump test, the launcher was operated at energies comparable to those in the jump test. The film, at 12,000 frames per second, does not reveal any relative motion between the plate edge and the stationary reference bar. Therefore, the muzzle motion during the shot is negligible.

For the evaluation of launch dynamics, an aim point and intended line of flight (LoF) were established by using a boresight. The bore sight is inserted in the muzzle end of the launcher and the crosshair indicated on the target with the eyepiece oriented in the vertical plane. However, since the boresight is referenced to the bore surface, some misalignment can exist because of the deviations of the bore centerline and surfaces. Also, the boresight is spring loaded to fit tight against the bore surface. This may be inadequate to accommodate changes in the bore surface or spring tension. To account for these errors, an optical telescope was used at the breech to indicate the bore centerline at two axial bore locations corresponding to where the sight contacts the bore surface near the muzzle. The optical telescope was then used to indicate a target 30 m down range. Geometry was used to convert the boresight reading taken at the muzzle to the actual LoF reading using the optical telescope. Additionally, the boresight was also repeatedly inserted and removed to assess its variability. It was found that the standard deviation for the horizontal direction is 0.36 mil and 0.42 mil in the vertical direction. (One mil corresponds to 1 m of deflection per 1000 m of range.) To reference the launcher LoF to the x-rays, a steel cable was attached at the breech, pulled through the launcher, and suspended over a pulley 5 m down range. The pulley was aligned with the boresight crosshair. The cable, for indicating LoF, and beads, for referencing the subprojectile cg location, were superimposed upon each x-ray. The LoF was corrected for misalignment with the boresight reading in the x-ray data reduction software.

Yaw cards (cardboard targets) were consistently used to assess the free-flight aerodynamics of the projectile. Seven yaw cards were placed at measured intervals along the first 40 m of trajectory. New yaw cards were put up before each shot and the yaw card located at 40 m was indicated with the boresight. The length of the subprojectile impact and the angular orientation relative to a vertical reference line was recorded. The pitch, yaw, and angle of attack (AoA) can then be determined from geometry. The flight range was 222 m. A 5-m-wide \times 5-m-high \times 20-mm-thick steel plate was used as an impact target. Additionally, a 1-m \times 1-m \times 178-mm thick armor plate was placed in front

of the impact target to acquire penetration data.

III. FREE-FLIGHT DATA AND ANALYSIS

In this study, free-flight angular motion of the subprojectile has been measured using the yaw cards placed along the flight path. The measured angular motion was then fitted to a theoretical model of the yawing motion, which is based on an analytical solution of the yawing motion of a rolling symmetric missile.[4] From the theoretical model, it is possible to extract information about the aerodynamic performance of the subprojectile and quantify the disturbances to the subprojectile during the launch and sabot discard process which establish the initial conditions for the free-flight angular motion. This information is then used to evaluate aspects of the transitional ballistics which effect the accuracy and dispersion of the subprojectile. The application of this technique is discussed in detail in a prior study.[4]

For this jump test, radar was used to obtain the velocity as a function of range. From these data, the subprojectile's drag coefficient (C_D) was obtained. This value also contains any additional effect from the subprojectile's average AoA. Since the launch velocity was held fixed for the jump test, the zero-yaw coefficient of drag is obtained from a plot of the C_D versus AoA squared as 0.397. This value is larger than but consistent with previously published theoretical results.[4] The discrepancy is attributable to the grooves along the rod body in the actual subprojectile.

IV. JUMP

In this section, the series of six disturbances from shot start to the impact of the round at the target (TI) are discussed. Jump is a vector, the sum of whose horizontal and vertical components is equal to the linear deviation from the line of fire produced by forces acting on the ILP. These angular displacements are typically expressed in mils. The first component is the pointing angle of the muzzle at projectile exit (PA). At the same time, the muzzle experiences a transverse velocity that is imposed upon the projectile (CV). The third component is the angular deviation of the projectile

cg from the instantaneous bore centerline at projectile exit (CG). The next component is the net deviation attributable to sabot discard disturbances (SD). The fifth jump component is the aerodynamic jump (AJ). The final jump component, GD, is the displacement attributable to gravity (g). Each jump component has a dispersion associated with it. If the individual jump components are independent of each other (i.e., no cross-correlation) and the data are normally distributed (in a statistical sense), the square root of the sum of the individual jump dispersions squared should equal the target impact dispersion (TID). Differences are attributed to measurement errors and cross-correlation. A thorough discussion of projectile jump and its measurement is presented in the literature.[6]

A. Linear Rates

Each of the jump components are deduced using a variety of existing transitional ballistics measurement techniques. For the present test, it is assumed that CV and PA vectors are negligible because the muzzle motion has been shown to be negligible for this particular launcher. The CG vector is determined from the location of the subprojectile's cg from the fiducial in the multistation orthogonal x-rays. A straight line is fit to the cg locations as a function of range for each plane and the slope of the line is the CG vector. The first three x-ray stations are used to determine the CG vector.

The last three x-ray stations are used to determine the final deflection of the subprojectile's trajectory prior to entering free-flight. This deflection is determined from the slope of a straight line fit to the cg displacements from the final three x-ray stations. The SD jump is assumed to occur after the CG jump and prior to the subprojectile entering free-flight. Hence, the SD vector is determined from the difference between the deflection measured from the last three x-rays and the deflection attributable to the CG vector. An example of the x-ray data taken on shot 12 is shown in Fig. 3.

Once the subprojectile enters free-flight, it is subjected to aerodynamic forces which may further deflect the flight trajectory of the subprojectile. The deflection due to the aerodynamic forces can be decomposed into mean and fluctuating components. The mean component is referred

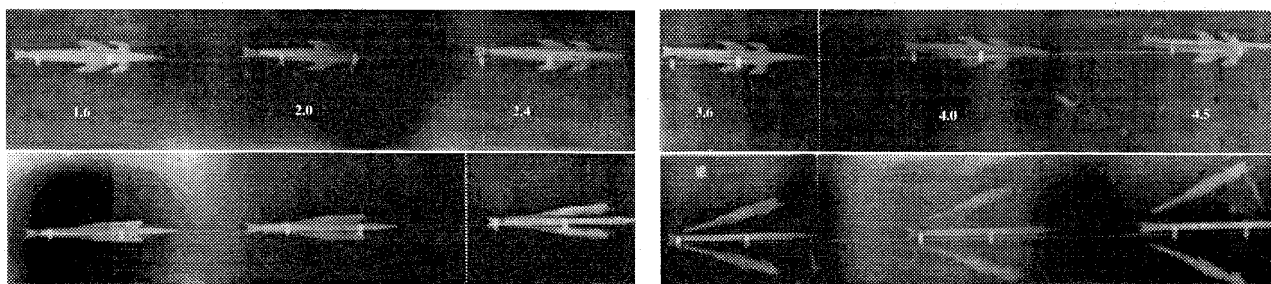


Fig. 3. Downrange orthogonal x-rays (shot 12). Units are in meters.

to as aerodynamic jump and it is produced by the angular rates as the round enters free flight. These rates cause a linear deviation of the mean trajectory from the original line of fire. The exact location where the subprojectile enters free-flight is somewhat ambiguous and, in this paper, it is taken to be 3.1 m down range. This is partly based on the flash x-ray images that show the armature disengaging from the subprojectile. Also, as in previous work, free-flight is determined by fitting a line to the lateral armature displacement data during discard and extrapolating to zero displacement. A reasonable approximation for AJ in mils [4] is given as

$$AJ = -1000 \frac{I_t C_{L\alpha}}{m d C_{m\alpha}} \delta' \quad (1)$$

The subprojectile moment of inertia (I_t), diameter (d), mass (m) and $C_{m\alpha}$ were measured. $C_{L\alpha}$ is obtained from CFD computations. The angular rate in rad/m, δ' , was determined for each plane, 3.1 m down range (i.e., free-flight), from the fits to the yaw card data.

In addition to the mean deflection of the trajectory, the projectile's swerving motion also has a fluctuating component, s , produced by the aerodynamic forces associated with the yawing motion of the round. These deflections are typically small and are usually not considered in a jump test where the yaw card targets are many yaw cycles from the muzzle of the gun. Since the impact data used to evaluate the jump components in the present test are taken after approximately one cycle of yawing motion, the fluctuating part of the swerving motion is included. This term represents an additional displacement for each plane along the trajectory. The fluctuating part of the swerving motion can be determined by integrating the equations of motion using the predicted lift coefficient, $C_{L\alpha}$, and the measured yawing motion. The resulting swerving motion is a damped periodic and is accounted for in the jump diagram by correcting the impact location. Fig. 4 shows the

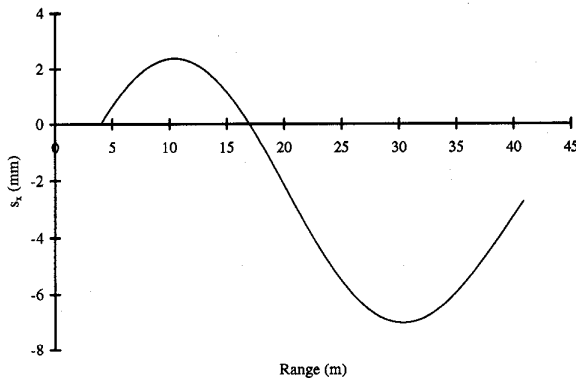


Fig. 4. Fluctuating part of free-flight swerving motion of subprojectile in the horizontal plane, shot 11.

computed fluctuating component of the swerving motion of the projectile for one of the shots in the test program. The subprojectile's yaw is close to a minimum at the 40 m yaw card which minimizes the impact of the displacement due to the fluctuating part of the swerving motion on the jump diagram.

Finally, the GD component, which only appears in the vertical displacement, has been computed in mils from the launch velocity (V) and range (Z) as

$$GD = 1000 \frac{gZ}{2V^2} \quad (2)$$

Fig. 5 shows a four-component jump vector diagram using impact data at 40 m down range for shot 8. The four components evaluated are CG, SD, AJ, and GD. The aim point is located at (0,0), and the impact at the target, denoted TI, has been corrected for the fluctuating part of the swerving motion. Similar plots were made for all the shots. Once the jump vector diagram is assembled, each vector is referenced from the origin. The variability of the vectors for each component is computed as the component dispersion. It is important to realize that the summation of the jump vectors should end at the impact location (i.e., closed). This assumes that all sources of error are accounted for in the analysis. For example, the impact location is known relative to the bore centerline to within the variability of the boresight. It is unreasonable to hold the impact location as a known error-free datum.

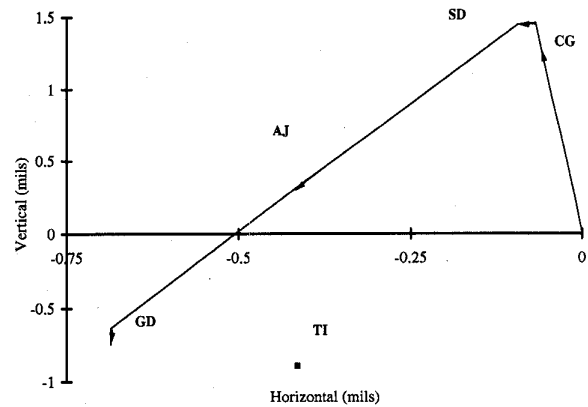


Fig. 5. Jump vector diagram for shot 8.

Fig. 6 shows the linear fit to the horizontal x-ray displacement data for two cases. In the first case, the impact location at 40 m is used, with corrections for AJ and s , to determine the (CG+SD) vector. This is equivalent to closing the jump diagram with the impact location. However, the boresight has a dispersion as indicated by the error bars. In the second case, only the last three x-ray displacement data are used to compute the final trajectory out to 40 m. The fit extrapolated to 40 m just lies within the impact location and the error of the boresight. If a normally distributed measurement error on the x-ray film is assumed to be ± 0.5 mm, then the agreement at 40 m

can be made much better. The dispersion at the yaw card is +18.5 mm, -20.4 mm. For all shots, an average of 4 mm is needed in the horizontal direction and 15 mm in the vertical direction for the trajectory based on the x-ray data to be within the impact location determined by the boresight. Therefore, based on the boresight variability and x-ray measurement accuracy, the jump diagrams are considered "closed" for each shot and no additional vectors are added to the existing components in order to close with the measured target impact location.

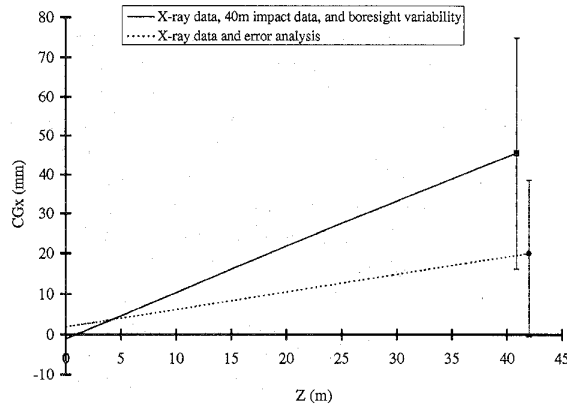


Fig. 6. Fitted linear displacements with boresight variability (solid) and x-ray error analysis (dashed) for shot 8, horizontal direction.

B. Dispersion

In Fig. 7, the dispersions for the CG, SD, and AJ jump components are plotted for the horizontal and vertical directions. The component dispersions are larger in the vertical direction than in the horizontal direction. This was also observed in previous work. However, the dominant contribution in the vertical

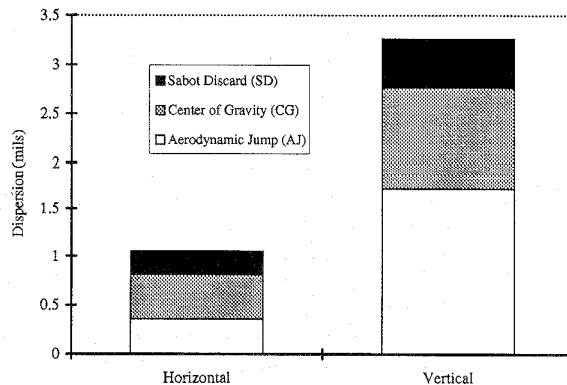


Fig. 7. Individual jump component dispersions.

direction is from the aerodynamic jump while in the horizontal direction it is attributable to in-bore balloting.

The impact locations at the 40 m and 222 m targets were used to compute the target impact dispersion (TID) which did not agree. This is significant since the TID is independent of reference location and should agree at both downrange locations. This suggests that the flight path was externally altered after the 40-m yaw card. Likely mechanisms include wind and subprojectile drift. Since the subprojectile does not incorporate any mechanism that produces spin to average any manufacturing asymmetries, drift is assumed. Also, based on the aerodynamic fits to the yaw card data, the subprojectile is reasonably stable and the planar motion decays as the round flies down range. The impact data used to determine the TID consisted of impact locations 40 m down range in azimuth and elevation. The impact data are corrected for the misalignment in the LoF.

Shown in Fig. 8 is the TID at 1,350 m/s with the insulated front contact armature. The variability in the boresight is accounted for in determining the TID. Also plotted is a fit to the previously published TID data in which a conducting front contact armature and different launcher were used.[4] Impact data for downrange locations less than 50 m are considered. It is clear that smaller dispersion was obtained in the horizontal direction as compared to previous results. The dispersion is 0.75 mil. However, only a slight decrease in dispersion is realized in the vertical direction. The dispersion is 2.74 mil. These results can be qualitatively explained by considering the launcher straightness. The IFC primarily affects the dynamics in the vertical direction. The launcher used in this present work has a more severe centerline profile than that used previously. If a CFC configuration had been used, the linear and angular rates from the muzzle would have been larger and therefore increased the TID. In the horizontal direction no modifications were made

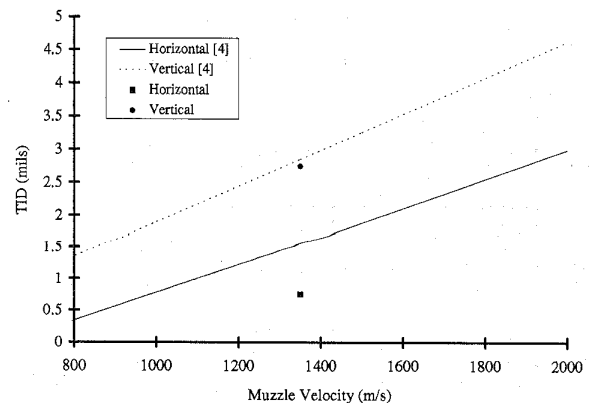


Fig. 8. Target impact dispersion as a function of launch velocity. Fit to previously published results for impacts less than 50m range and data from this investigation.

in the ILP. The reduced dispersion is most likely a result of cross-correlation with the SD jump component and a slightly less severe straightness in the horizontal plane.

The horizontal and vertical TIDs, based on a linear summation of the jump vectors and no cross-correlation, are 0.62 and 2.07 mils and are quite reasonable in comparison to the TID measured at the 40 m yaw card target. This is encouraging since the calculations for the jump vectors do not rely on the target impact location data.

C. Angular Rates

The angular rates determined by the first three x-rays are indicative of the in-bore balloting forces acting on the ILP cg. The angular rates associated with free flight are also a result of the armature discard event and represent the final angular motion of the round.

The free-flight angular rates are larger than the rates measured in previous tests. The average magnitude of the free-flight angular rate is $1.72^\circ/\text{m}$ in the horizontal and $0.63^\circ/\text{m}$ in the horizontal direction. On average, the rates representative of in-bore balloting contribute 65% toward the free-flight rates. The dominant component in the vertical direction is associated with AJ. This is consistent with the larger TID in elevation and the bore straightness profile. Similarly, the angular rates are lowest in the horizontal direction. In previous work, the most significant contribution to the free-flight angular rate was produced by the sabot discard.

V. SUMMARY

Results indicate the weapon designer's ability to enhance the accuracy and dispersion of an electromagnetic gun. The improved TID in the horizontal direction is a result of a slightly better launcher straightness compared to that in previous work. Also, the tests reported here used an armature current profile that previously demonstrated a slight improvement in subprojectile accuracy.[2] This acceleration profile was consistently used in this jump test.

The linear and angular rates produced by the launcher appear to be the major contributor to the TID. The dominant linear rate for both planes is produced by the launcher (CG). The linear rates were effectively managed by the use of a less stiff front armature contact.

The angular rates produced by the launcher contribute significantly toward the free-flight rates. These rates manifest themselves as a linear displacement in the aerodynamic jump (AJ). These rates are managed in the subprojectile by the pitching moment coefficient. The goal of further enhancing the accuracy is then to balance the contribution of the linear and angular rates through armature and subprojectile design changes so that the net contribution toward TID is minimized.

There is opportunity in the current experimental procedure to improve the measurement accuracies. For example, the boresight could be designed to improve its measurement fidelity. Alternatively, another measurement technique could be developed to indicate the line of flight. Although a direct result would be improved accuracy for TID, the (CG+SD) jump vector could be better defined when the target impact location is used in the data reduction. Further improvements in the x-ray measurements are desired to reduce variability in determining the CG and SD jump components. These include optimum downrange location of the x-ray images and larger magnification factors. These improvements are necessary to evaluate cross-correlation effects between the jump components and will certainly be required as the accuracy of the round improves. However, for the current round, the measurement accuracies are sufficient to characterize the total jump and the contribution from each jump component.

REFERENCES

- [1] H. D. Fair, "Electromagnetic launch: a review of the U.S. national program," *IEEE Trans. Magn.*, vol. 33, no. 1, pp. 11-16, January 1997.
- [2] A. E. Zielinski, P. Weinacht, and J. P. Powell, "Effect of rail-gun electrodynamics on ballistic performance," U.S. Army Research Laboratory, Technical Report in review. Aberdeen Proving Ground, MD, 1998.
- [3] A. E. Zielinski, and M. D. Werst, "Cannon-caliber electromagnetic launcher," *IEEE Trans. Magn.*, vol. 33, no. 1, pp. 630-635, January 1997.
- [4] A. E. Zielinski, P. Weinacht, D. W. Webb, and K.P. Soencksen, "An investigation of the ballistic performance for an electromagnetic gun-launched projectile," ARL-TR-1361, U.S. Army Research Laboratory, Aberdeen Proving Ground, MD, June 1997.
- [5] A. E. Zielinski and D. Hildenbrand, "Observation and simulation of armature contact performance in the cannon-caliber electromagnetic gun," *IEEE Trans. Magn.*, vol. 33, no. 1, pp. 157-162, January 1997.
- [6] J. Bornstein, I. Celmins, P. Plostins, and E. M. Schmidt, "Techniques for the measurement of tank cannon jump," BRL-MR-3715, U.S. Army Ballistic Research Laboratory, Aberdeen Proving Ground, MD, December 1988.

ACKNOWLEDGMENT

Funding for this effort was provided by ARL Electric Armaments Program Office. Significant contributions, in support of the experimental results, were made by Mr. Ken Paxton, Mr. Barry Hudler, Mr. Brendan Patton, and Mr. Donald "Mac" McClennan. The bore straightness measurements were provided by Mr. Terri Marrs, Aberdeen Test Center. Statistical support was provided by Mr. Dave Webb, ARL. The ILPs were generously provided by CEM-UT through the Close Combat Armaments Center, ARDEC Picatinny NJ.